Supporting Information

Oxygen-Vacancy Rich in Melilite to Modulate the Persistent Luminescence for Multi-Functional Application

Youchao Kong[1], Shurong Chen[2], Jie He[2], Shuwei Deng[2], Xiaoshuang Li[2*] and Jiangcong Zhou[3*]

[1]Department of Physics and Electronic Engineering, Yancheng Teachers University, Yancheng 224002, P.R. China

[2]School of Applied Physics and Materials, Wuyi University, Jiangmen, Guangdong 529020, P.R. China

[3]College of Chemistry & Materials Science, Longyan University, Fujian, 364000, P.R. China

Corresponding author.

E-mail address:

Xiaoshuang Li: lixiaoshuang12@mails.ucas.ac.cn

Jiangcong Zhou: jiangcongzhou@163.com;

Experimental section:

Sample preparation

All phosphors were synthesized using a traditional solid-state method. The raw materials were $CaCO_3$ (99.99%), MgO (99.99%), SiO_2 (A.R.), and Eu_2O_3 (99.99%), which were used directly without any further treatment. The stoichiometric starting materials were thoroughly homogenized, the mixture was transferred into an alumina crucible and then loaded into a muffle furnace. Then the mixed samples were sintered at 1150 °C for 5 h under 95% N_2+5% H_2 reductive atmosphere. The obtained samples were cooled to room temperature and then ground again in an agate mortar. Finally, the solid powder samples were sintered at 550 °C in H_2 for 1h, 3h and 5 h to obtain the V_O-CMSE for subsequent analysis and measurements.

Characterization

The powder X-ray diffraction (PXRD) patterns of the as-obtained samples were collected on a X' Pert PRO diffractometer (Cu Kα radiation, λ = 1.5406 Å) at 298 K. The microstructure was analyzed using a scanning electron microscope (SEM, JSM-6700F) and transmission electron microscope (FE-TEM, JEM-2100F, JEOL). The X-ray photoelectron spectroscopy (XPS, Thermo fisher Scientific K-Alpha) was conducted to identify the chemical states of the elements in the sample. A FLS-980 fluorescence spectrophotometer (Xe 900, 450 W arc lamps) was employed to obtain the photoluminescence (PL), photoluminescence excitation (PLE), and decay curve spectra. An absolute photoluminescence quantum yield measurement system (Hamamatsu, Quantaurus-QY plus C13534-31) was adopted to test the quantum

efficiency. A LTTL-3DS measurement was used to record the 3D TL glow curves at a heating rate of 2 K•s^{-1}.

Computational methods：

Utilizing density functional theory (DFT) as implemented in the Vienna *ab-initio* simulation package code,[1] we investigate the electronic structures of title compound. We used projector augmented wave (PAW) method[2] for the ionic cores and the generalized gradient approximation (GGA) for the exchange-correlation potential, in which the Perdew-Burke-Ernzerhof (PBE) type[3] exchange-correlation was adopted. The reciprocal space was sampled with 0.03 Å^{-1} spacing in the Monkhorst-Pack scheme for structure optimization, while denser k-point grids with 0.01 Å^{-1} spacing were adopted for properties calculation. We used a mesh cutoff energy of 400 eV to determine the self-consistent charge density. All geometries are relaxed until the Hellmann-Feynman force on atoms is less than 0.01 eV/Å and the total energy change is less than 1.0×10^{-5} eV. The calculation models were built from the crystal structure. To calculate the formation energy of oxygen vacancies, the following equation was used: Evac = E(slab+Ovac) - E(slab) - E(O). Here, E(slab+Ovac), E(slab), and E(O) denote the energies of the surface with one oxygen vacancy, the clean surface, and the isolated oxygen atom, respectively.

[1] A. G. Kresse, J. Furthmüller, Efficient iterative schemes for ab initio total-energy calculations using a plane-wave basis set. Phys. Rev. B 1996, 54, 11169.

[2] B. G. Kresse, J. Furthmüller, Efficiency of Ab-initio total energy calculations for metals and semiconductors using a plane-wave basis set. Com. Mater. Sci. 1996, 6, 15-50.

[3] J. P. Perdew, K. Burke, M. Ernzerhof, Generalized gradient approximation made simple. Phys. Rev. Lett. 1996, 77, 3865.
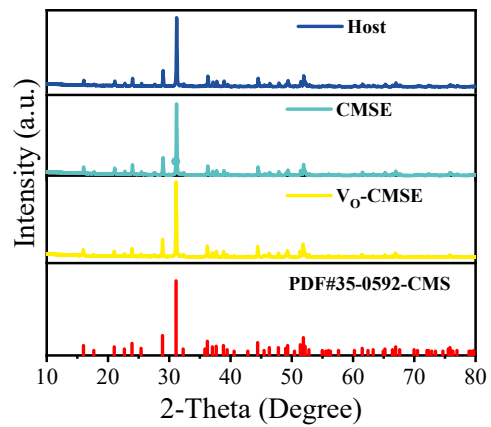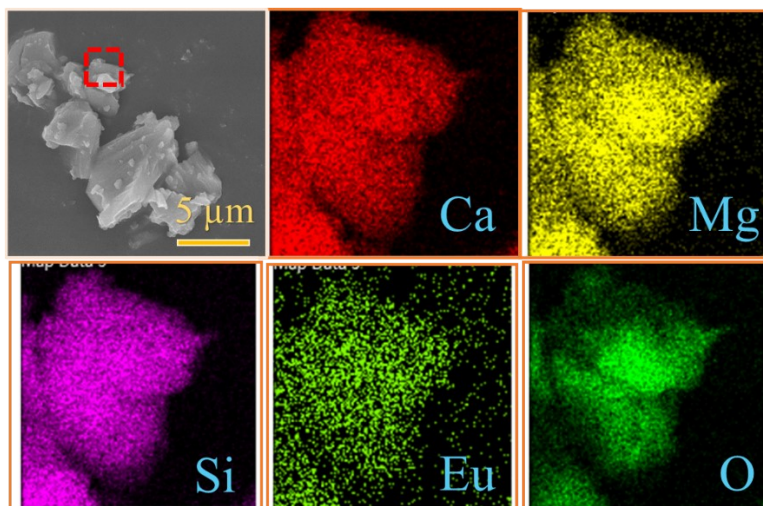
Fig. S1 Powder XRD patterns of CMSE and V_O-CMSE.
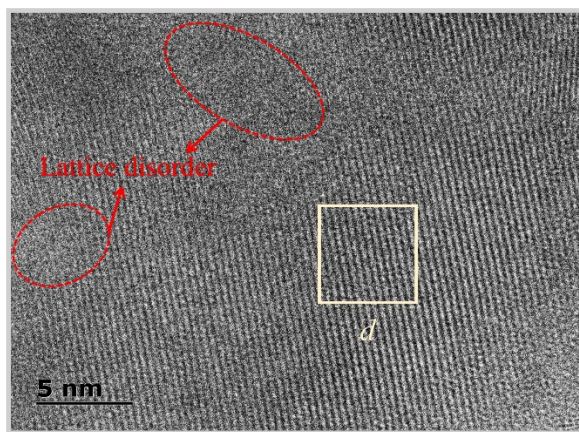
Fig. S2 SEM and EDS element mapping images of V_O-CMSE.

Fig. S3 High-resolution TEM image of V_O-CMSE, the lattice disorder induced by defects is marked by red arrows.
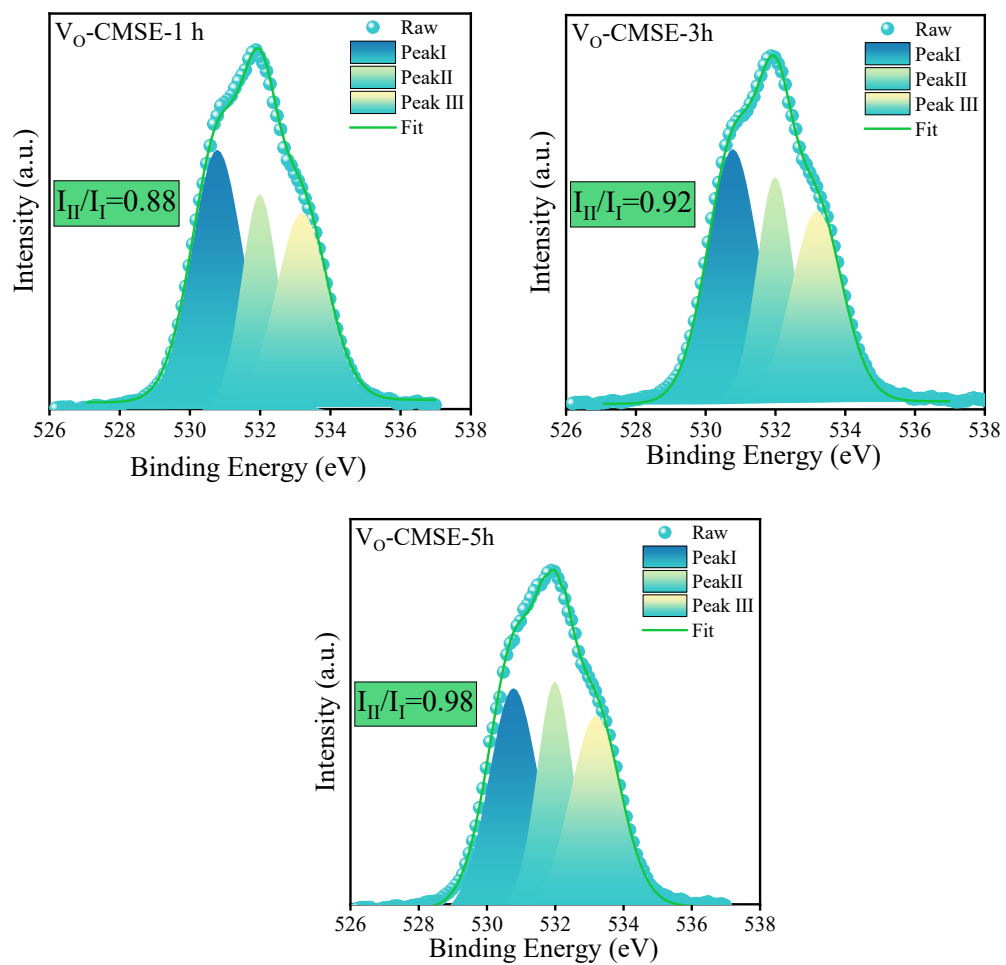
Fig. S4. Fitted O 1s XPS spectra of CMSE under various treatment time.
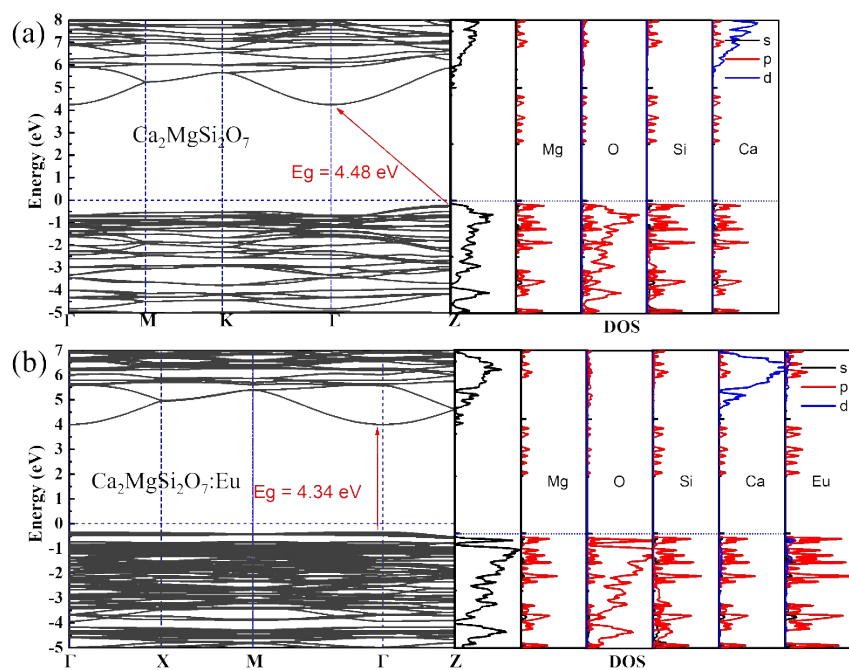
Fig. S5 Bandgaps and DOSs of CMS and CMSE.
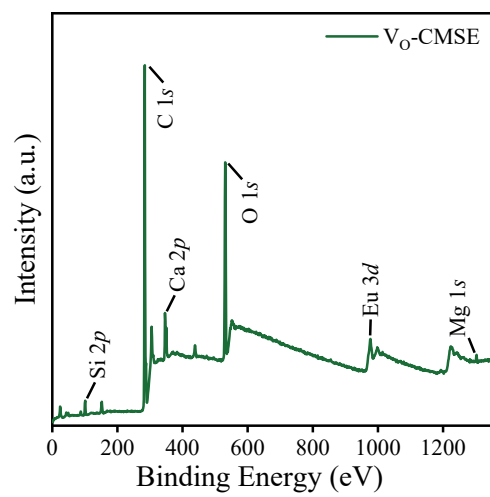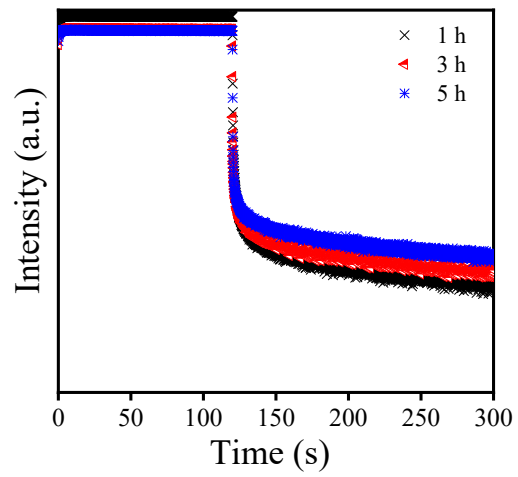
Fig. S6 XPS spectrum of V_O-CMSE.

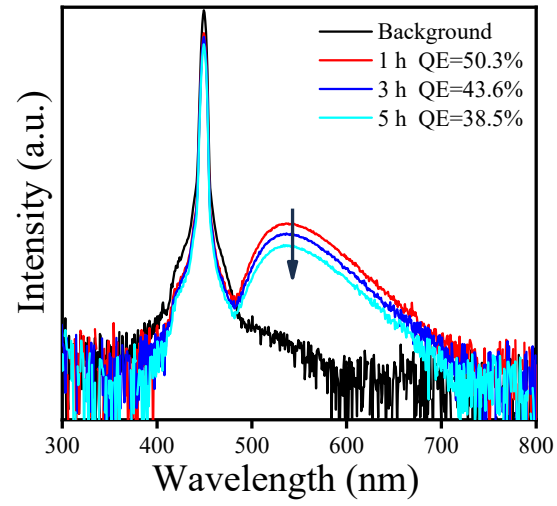**Fig. S7** PersL decay curves of V_O-CMSE under various treatment time.
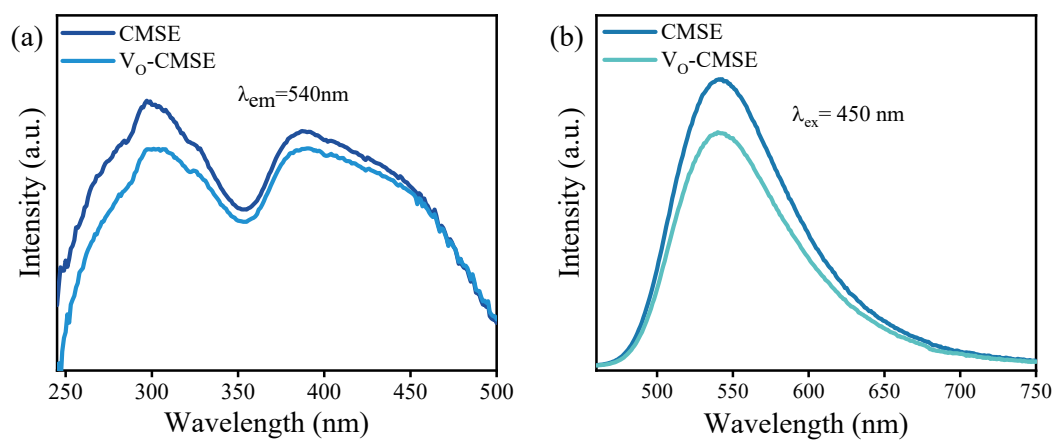
Fig. S8 The IQE value of VO-CMSE under 450 nm excitation.
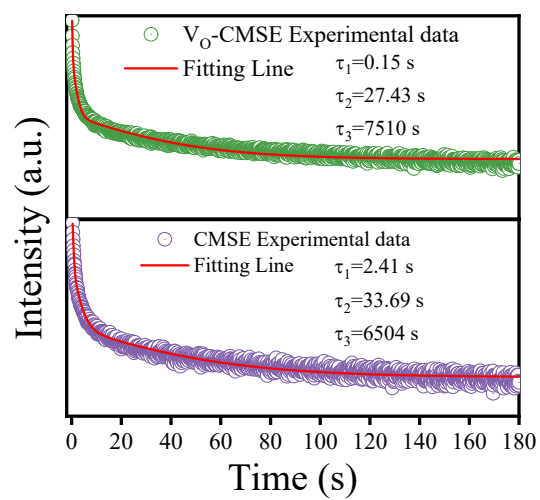
Fig. S9 PLE and PL spectra of CMSE and V_O-CMSE.
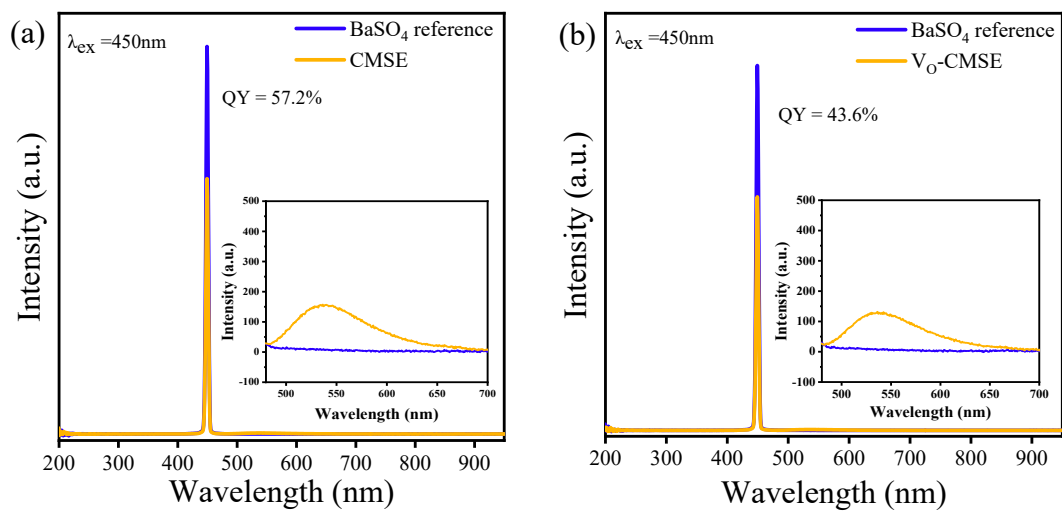
Fig. S10 PersL decay curves of CMSE and V_O-CMSE.

Fig. S11 QE values of CMSE and V_O-CMSE.
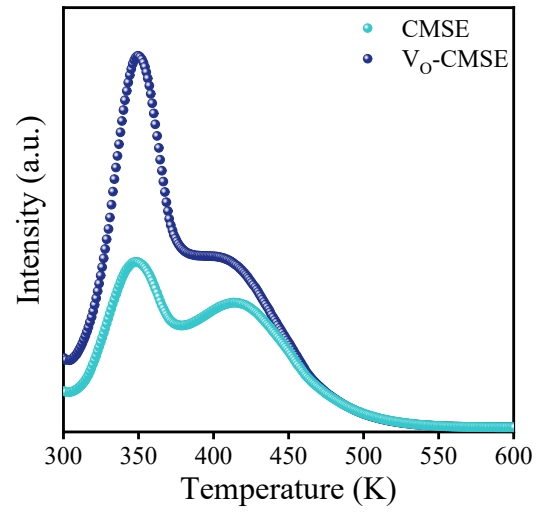
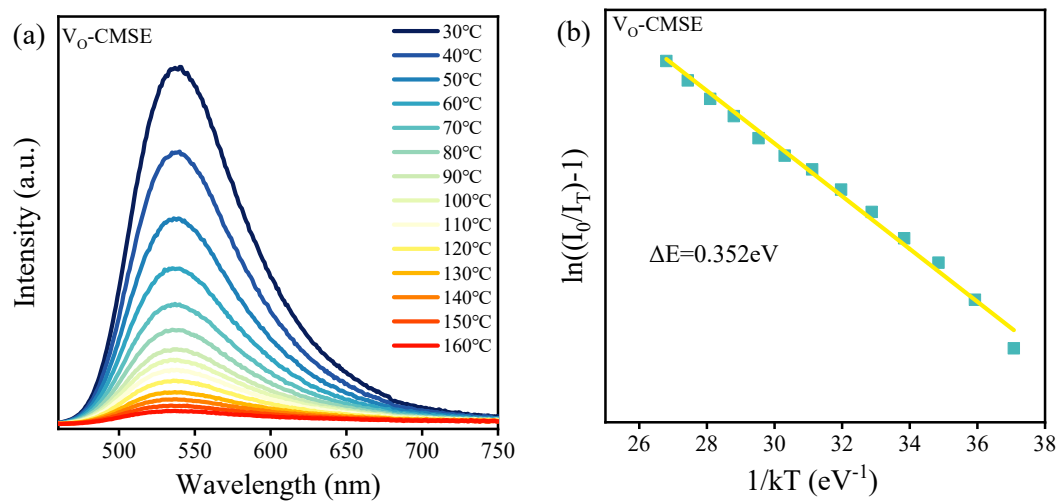**Fig. S12** TL spectra of CMSE and V_O-CMSE.

Fig. S13 (a) Temperature dependent PL of V_O-CMSE. (b) The calculated Ea value.